



Acoustic tunneling through artificial structures: From phononic crystals to acoustic metamaterials

Pai Peng^a, Chunyin Qiu^{a,*}, Yiqun Ding^a, Zhaojian He^a, Hai Yang^b, Zhengyou Liu^a

^a Key Laboratory of Artificial Micro- and Nano-structures of Ministry of Education and School of Physics and Technology, Wuhan University, Wuhan 430072, China

^b Physics Department, Yunnan Normal University, 650092, Kunming, China

ARTICLE INFO

Article history:

Received 3 September 2010
 Received in revised form
 28 November 2010
 Accepted 7 December 2010
 by X. Chen
 Available online 13 December 2010

Keywords:

A. Acoustic metamaterial
 A. Sonic crystal
 D. Tunneling

ABSTRACT

We present a comparative study on the acoustic tunneling through artificial periodical composites, from phononic crystals to acoustic metamaterials. We find that the features of the acoustic tunneling are closely related with the origins of band gaps. In particular, the band gap associated with the negative effective material parameter in the metamaterial results in a better analog of the tunneling effect to the quantum system.

Crown Copyright © 2010 Published by Elsevier Ltd. All rights reserved.

1. Introduction

The propagation of acoustic waves in phononic crystals (PCs) has aroused much attention in past decades [1–8]. Besides these investigations closely related with the applications on sound [1–5], such as sound insulation [1], acoustic wave guides [2] and filters [3], acoustic lenses [4,5], and so on, much effort has been devoted to study the fundamental physics that exhibits the common features of the waves coupling with structures. Analog to the situation for electrons in crystalline solids, the Bloch oscillation, Zener tunneling, and Zitterbewegung phenomena have been observed for acoustic waves in PCs [6–8]. In fact, in contrast to the electron systems, the macroscopic characteristics of the acoustic systems (with typical length scale in millimeters and time scale in microseconds) could greatly benefit the experimental measurement through the sophisticated ultrasonic scanning technique [5–8].

Tunneling is one of the most intriguing phenomena in quantum mechanics that continues to attract extensive interest up to now [9–11]. A striking character for the tunneling effect is that the group delay of the quantum particle shows an asymptotic saturation with increasing barrier thickness, implying a superluminal speed without causality violated. The tunneling phenomena are common for all waves that travel through a nominally forbidden region, e.g., electromagnetic waves propagating in the photonic

crystals with band gaps [12–15]. Similar studies have also been extended into the acoustic tunneling in PC systems [16,17]. Although a universal behavior is exhibited for the group velocity in these systems, there is a qualitative difference for the phase velocity: it grows linearly with the sample thickness for the quantum case, whereas it almost keeps invariant for the classical case. The difference comes from the distinct origins of the forbidden zones. For the quantum case, the forbidden zone corresponds to the evanescent potential barrier, while for the classical case it corresponds to the band gap resulting from Bragg scatterings [16].

Recently, another type of periodical composites, i.e., the so-called acoustic metamaterials are receiving growing attention within the physics community [18–23]. Different from the PC case whose band gaps occur at the wavelengths comparable with structural periods, the band gaps in metamaterials can be created in the long wavelength regime, which have been verified to be associated with negative effective material parameters. In this work, we give a comparative study on the acoustic tunneling between the PC and the metamaterial systems, and find that the phase velocity in the metamaterial behaves more alike with the quantum case since the band gap resembles the potential barrier, as shown below. By gradually adjusting the material properties of the composite, we also study the crossover behavior from the PC to the metamaterial.

The paper is organized as follows. In Section 2, we first give a simple review for the acoustic tunneling through a PC slab, and in Section 3 we present a comparative study for the case of the metamaterial. The crossover behavior is discussed in Section 4 and a conclusion is finally made in Section 5. Throughout the work, we employ the layer-multiple-scattering-theory (LMST) [24] method

* Corresponding author. Tel.: +86 13554342967.
 E-mail address: cyqiu@whu.edu.cn (C. Qiu).

to numerically calculate the phase and group velocities. For the metamaterial case, with retrieving the effective elastic parameters by the coherent-potential approximation (CPA) method [20–22], in the Appendix we also provide the corresponding analytical results, which are in excellent agreement with the numerical ones.

2. Acoustic tunneling through PC slabs

Here we give a simple review for the acoustic tunneling through a PC made by pure solid components and consider only the longitudinal incident waves. The PC consists of a simple cubic array of steel beads embedded in epoxy, where the lattice constant is a and the radius of the steel bead is $0.25a$. The material parameters used are $\rho_0 = 1.18 \times 10^3 \text{ kg/m}^3$, $\lambda_0 = 4.43 \times 10^9 \text{ N/m}^2$ and $\mu_0 = 1.59 \times 10^9 \text{ N/m}^2$ for epoxy; $\rho_1 = 7.9 \times 10^3 \text{ kg/m}^3$, $\lambda_1 = 1.1 \times 10^{11} \text{ N/m}^2$, and $\mu_1 = 8.2 \times 10^{10} \text{ N/m}^2$ for steel. Here ρ is the mass density, and λ and μ are the elastic and shear moduli, respectively.

Without data presented here, both the band structure and the transmission spectrum along [100] direction indicate a longitudinal band gap from the normalized frequency $\omega_L \simeq 0.30$ to $\omega_U \simeq 0.37$. Within the band gap the propagation of acoustic waves is prohibited when the system is infinitely large. For a PC slab of finite thickness L , however, the acoustic signal can tunnel through it at low transmittance. From the transmission coefficient calculated by the LMST method, it is easy to extract the frequency dependent phase difference ϕ between the transmitted and incident waves at the both surfaces, which determines the phase velocity $V_p = \omega/k = \omega L/\phi$ and the group velocity $V_g = d\omega/dk = Ld\omega/d\phi$ [16].

Fig. 1(a) shows the frequency dependent accumulative phase difference for a 40-layer PC slab. It increases monotonically with frequency and varies continuously at the both band edges. Because of the cancellation of Bragg scatterings, inside the band gap the real part of the wave vector $k_R = \pi/a$ [22,25], and hence the accumulative phase difference is almost (yet not) a constant, i.e., $\phi \simeq k_R L = 40\pi$. As a consequence, the phase velocity within the band gap can be simply estimated by $V_p \simeq \omega a/\pi$ and follows a linear dependence with the frequency, as shown in Fig. 1(b). As for the group velocity V_g (at the given sample thickness), near the band edges it is very slow, and away from the band edges it grows quickly and even exceeds the velocity of sound in the background [see Fig. 1(c)]. In fact, as indicated in Fig. 2 by the linear dependence on the slab thickness, the group velocity within the band gap can be extremely high. This is in contrast to the (frequency dependent) phase velocity, which almost keeps invariant as the slab thickness increases.

3. Acoustic tunneling through metamaterial slabs

Now we consider a three-component system consisting of a simple cubic array of silicon–rubber-coated steel beads embedding in epoxy, where the inner and the outer radii of the soft coating-layer are $0.25a$ and $0.35a$, respectively. The sample is identical to the above PC except that a thin layer of epoxy is replaced by the soft silicon–rubber (with material parameters $\rho_2 = 1.18 \times 10^3 \text{ kg/m}^3$, $\lambda_2 = 4.43 \times 10^5 \text{ N/m}^2$ and $\mu_2 = 1.59 \times 10^4 \text{ N/m}^2$). In this system, the strong local (dipolar) resonance of the individual multi-component unit may create band gaps at very low frequencies [20,21], which is different from the PC case with band gaps resulting from the collective Bragg scatterings. Since the wavelength concerned here is much larger than the characteristic structural lengths, the system can be viewed as a homogenous material and the effective parameters can be retrieved, such as by CPA method [20–22]. In particular, the lowest band gap occurs from $\omega_L = 3.0 \times 10^{-3}$ to $\omega_U = 3.6 \times 10^{-3}$, within which the elastic

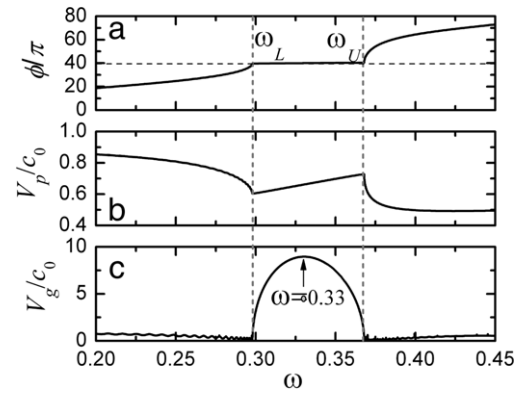


Fig. 1. (a) The accumulative phase difference ϕ , (b) the phase velocity V_p , and (c) the group velocity V_g for a 40-layer PC slab plotted as a function of the normalized frequency (in unit of c_0/a , with a being the lattice constant and c_0 being the longitudinal wave velocity in the background). Here the vertical dashed lines denote the positions of the upper (ω_U) and the lower (ω_L) band edges.

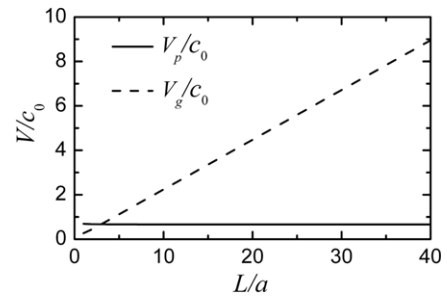


Fig. 2. The phase (solid line) and group velocities (dashed line) for a typical frequency ($\omega = 0.33$) within the band gap plotted as a function of the sample thickness.

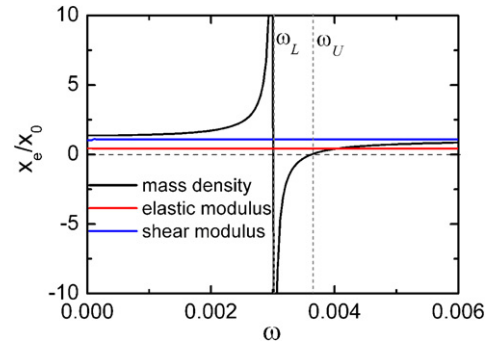


Fig. 3. (Color online) Frequency dependent effective elastic parameters X_e of the metamaterial normalized by those in the background X_0 , with the vertical dashed lines denoting the band edges.

and shear moduli keep normal whereas the mass density turns effectively negative, as shown in Fig. 3. Based on these effective parameters, the accumulative phase difference, phase and group velocities can be obtained in an analytic way (see Appendix). As to be shown in Figs. 4 and 5, the analytic results (solid lines) agree well with the numerical data (dashed lines).

In Fig. 4 we show the frequency dependencies of the accumulative phase difference ϕ , phase velocity V_p and group velocity V_g for a 1000-layer metamaterial slab. Besides the lowest band gap, we also present the data for the adjunctive pass bands where all of the effective material parameters are positive. As the frequency goes up to the lower band edge ω_L , due to the fast growth of the (positive) effective mass density (see Fig. 3), the effective longitudinal wave velocity of the metamaterial reduces, and the wave vector and hence the accumulative phase difference increases rapidly.

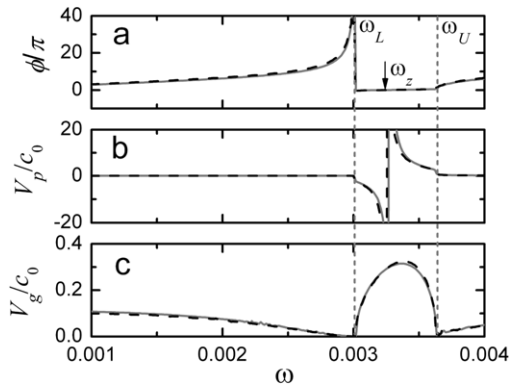


Fig. 4. Frequency dependencies of (a) the accumulative phase difference, (b) the phase velocity, and (c) the group velocity for a 1000-layer sample, with solid and dashed lines denoting the analytic and numerical results, respectively. Here the vertical dashed lines denote the band edges and the arrow denotes the frequency ω_z with $\phi = 0$.

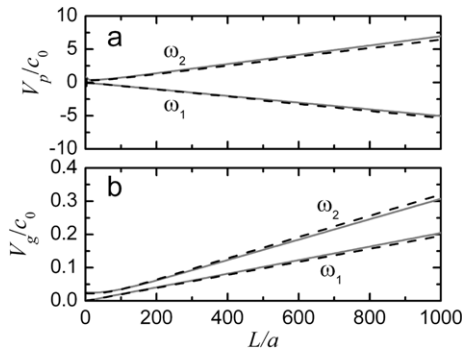


Fig. 5. Sample thickness dependencies of (a) the phase velocity and (b) the group velocity at two typical frequencies inside the band gap, with solid and dashed lines denoting the analytic and numerical results, respectively.

Within the band gap, the acoustic wave tunnels through the metamaterial slab with decaying amplitude since the effective wave vector becomes purely imaginary. The finite value of ϕ is induced by the boundary effect and the finite thickness of the slab. As predicted in the Appendix, ϕ and hence V_p could be either positive or negative. In addition, at the normalized frequency $\omega_z \simeq 3.2 \times 10^{-3}$, $\phi = 0$ and V_p diverges. Such a discontinuity of V_p within the band gap is absent in the PC case. As for the group velocity V_g , it is almost zero at the band edges and reaches its maximum at the frequency near the center of the band gap, similar to the PC case [see Fig. 1(c)].

Fig. 5 shows the thickness dependencies of the phase and group velocities for two typical frequencies on the both sides of ω_z , $\omega_1 = 3.1 \times 10^{-3}$ and $\omega_2 = 3.4 \times 10^{-3}$. It is observed in Fig. 5(a) that the phase velocity increases (or decreases) monotonically with the sample thickness and quickly approaches to a linear behavior due to the saturation of the accumulative phase difference, as predicted in the Appendix by the Eqs. (A.5) and (A.6). This is in contrast to the PC case where the phase velocity is almost independent on the thickness [see Fig. 2]. As for the group velocity, it also exhibits a linear relationship with the slab thickness [see Fig. 5(b)], which is similar to the PC case. The linear behaviors of the both velocities in the metamaterial system arise from the similarity of the forbidden zone to the quantum system, as indicated in Eq. (A.9) in the Appendix.

4. Intermediate systems between the PCs and the metamaterials

The main difference of the acoustic tunneling between the PC and the metamaterial results from the distinct origins responsible

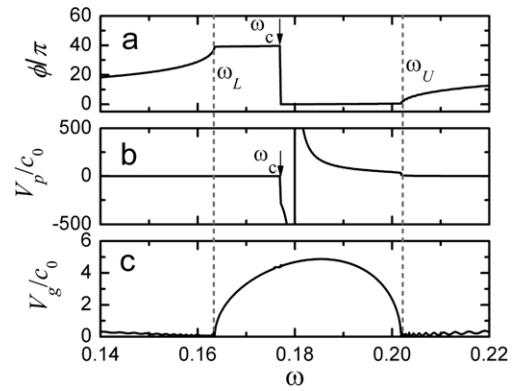


Fig. 6. Frequency dependencies of (a) the accumulative phase difference, (b) the phase velocity, and (c) the group velocity for a 40-layer sample with the parameter $p = 1500$. Here the vertical dashed lines denote the band edges and the arrows denote the critical frequency ω_c .

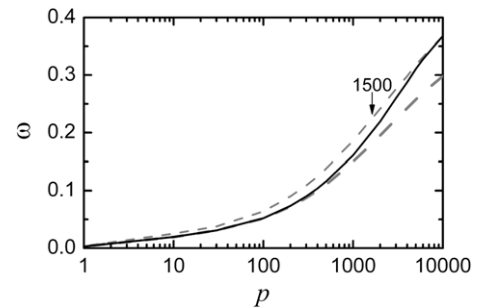


Fig. 7. The critical frequency ω_c (solid line) plotted as a function of the parameter p , with the dashed lines denoting the upper and the lower band edges.

for the band gaps: Bragg scattering for the former case and local resonance for the latter case. Now a natural question arises: how about the intermediate systems connecting these two cases?

For simplicity, we construct the intermediate system by using a single parameter p : $\lambda_m = p\lambda_2$, $\mu_m = \mu_0 + (\mu_0 - \mu_2)(p\lambda_2 - \lambda_0) / (\lambda_0 - \lambda_2)$, and $\rho_m \equiv \rho_0$ (note that we have already chosen $\rho_0 = \rho_2$ previously). Therefore, with p varying from 1 to 10 000, we can realize the metamaterials and PCs by adjusting the elastic properties of the coating layer.

Without losing generality, the parameter $p = 1500$ is used to exhibit the crossover behavior of the acoustic tunneling from the PC to the metamaterial. In Fig. 6(a) we display the frequency dependence of the accumulative phase difference ϕ around the first band gap for a 40-layer sample. It is observed that within the band gap there exists a critical frequency ω_c . Below ω_c , the phase difference is almost a constant ($\phi \simeq 40\pi$), similar to the PC case [see Fig. 1(a)]; above ω_c , it jumps to a small value and behaves as the situation of the metamaterial [see Fig. 4(a)]. Accordingly, this critical frequency is also characterized by a discontinuity in the phase velocity V_p , as shown in Fig. 6(b). The other discontinuity of V_p appears at a higher frequency (where $\phi = 0$), which is similar to the metamaterial case [see Fig. 4(b)]. It is of interest that there is no observable discontinuity occurring in the group velocity, as shown in Fig. 6(c).

The above analysis states that for the intermediate system the band gap can be divided into two frequency regimes that respectively correspond to the PC and the metamaterial. In fact, near the lower band edge the band gap always exhibits a character of Bragg type [22]. The critical frequency shifts from the lower band edge to the upper one as the coating layer becomes harder, and finally the whole band gap becomes a Bragg type, as shown in Fig. 7.

5. Conclusion

In this work, we present a comparative study for the acoustic tunneling through the PCs and metamaterials. For the PC case, the group velocity and the phase velocity exhibit different dependencies on the sample size: the former one grows linearly with the thickness as long as it is large enough, whereas the latter one almost keeps invariant. For the metamaterial case, the linear relationship holds for the both velocities, which resembles the quantum particle tunneling through a potential barrier. The different acoustic tunneling behaviors between these two types of artificial structures arise from the distinct origins for the band gaps, i.e., Bragg scattering for the PC whereas local resonance for the metamaterial. In addition, we have also studied the crossover behavior from the PC to the metamaterial by adjusting the material's parameters gradually. We find that there exists a characteristic frequency that divides the band gap into two different regimes, exhibiting either the PC-like or the metamaterial-like behaviors.

Acknowledgements

The work is supported by the National Natural Science Foundation of China (Grant No. 10874131); NSFC/RGC joint research grants 10731160613 and N_HKUST632/07; Hubei Provincial Natural Science Foundation of China (Grant No. 2009CDA151); National Natural Science Foundation of China for Less Developed Regions (Grant No. 10864009); and China Postdoctoral Science Foundation (Grant No. 20090460990).

Appendix

We consider a longitudinal acoustic plane wave e^{ik_0x} incident normally upon a homogenous slab (with boundaries defined by $x = 0$ and $x = L$) from a solid host material with positive material parameters. It is easy to deduce that the displacement at $x = L$ reads

$$u = \frac{4Z_A^2}{(Z_A + Z_B)^2 e^{-ik_B L} - (Z_A - Z_B)^2 e^{ik_B L}}, \quad (\text{A.1})$$

where Z and k represent respectively the longitudinal acoustic impedance and wave vector in the host material (A) and the slab (B). If all of the material parameters for the slab are positive, Z_B and k_B are purely real numbers and the accumulative phase (relative to the input wave at $x = 0$) reads

$$\phi = \arctan \left[\frac{Z_A^2 + Z_B^2}{2Z_A Z_B} \tan(k_B L) \right] + n\pi, \quad (\text{A.2})$$

with n being an integer.

When the mass density of the slab is negative, the longitudinal wave velocity and thus the acoustic impedance and wave vector become purely imaginary. By using the positive quantities $\tilde{k}_B = -ik_B$ and $\tilde{Z}_B = -iZ_B$, Eq. (A.1) can be rewritten as

$$u = \frac{2Z_A^2}{(Z_A^2 - \tilde{Z}_B^2) \sinh(\tilde{k}_B L) + i2Z_A \tilde{Z}_B \cosh(\tilde{k}_B L)}, \quad (\text{A.3})$$

and accordingly the accumulative phase difference

$$\phi = \arctan \left[\tanh(\tilde{k}_B L) (Z_A^2 - \tilde{Z}_B^2) / (2Z_A \tilde{Z}_B) \right], \quad (\text{A.4})$$

which determines the phase velocity $V_p = \omega L / \phi$ and the group velocity $V_g = L d\omega / d\phi$. It is of interest that V_p could be either positive or negative, depending on the sign of $Z_A - \tilde{Z}_B$, and it diverges when $\tilde{Z}_B = Z_A$ and $\phi = 0$.

The negative mass density, which is absent in nature, can be realized in acoustic metamaterials. For a sufficiently thick metamaterial slab ($L \gg \tilde{k}_B^{-1}$), $\tanh(\tilde{k}_B L) \rightarrow 1$ and ϕ approaches to a constant

$$\phi \simeq \arctan \left[(Z_A^2 - \tilde{Z}_B^2) / (2Z_A \tilde{Z}_B) \right], \quad (\text{A.5})$$

which provides the phase velocity

$$V_p \simeq \omega L / \arctan \left[(Z_A^2 - \tilde{Z}_B^2) / (2Z_A \tilde{Z}_B) \right], \quad (\text{A.6})$$

and the group velocity

$$V_g \simeq - \frac{(Z_A^2 + \tilde{Z}_B^2)L}{2Z_A (\partial \tilde{Z}_B / \partial \omega)}, \quad (\text{A.7})$$

both proportional L . This means that the phase time $t_p = L/V_p$ and the group time $t_g = L/V_g$ are both independent of the sample's thickness as long as it is large enough.

Similar phenomena have also been predicted for the electron tunneling through a potential barrier. For an electron of kinetic energy E incident upon a rectangular potential barrier with width W and height H ($H > E$), the phase difference between the transmitted and input waves [9,16]

$$\phi = \arctan \left[\frac{2E - H}{2\sqrt{(H - E)E}} \tanh(\tilde{k}W) \right], \quad (\text{A.8})$$

where $\tilde{k} = \sqrt{2m(H - E)/\hbar^2}$ is the amplitude of the purely imaginary wave vector inside the potential barrier, with m being the mass of the electron and \hbar being the reduced Planck constant. Compared Eq. (A.4) with Eq. (A.8), it is easy to find a mathematical mapping from the acoustic system to the quantum system:

$$\left[L, \tilde{k}_B, Z_A, \tilde{Z}_B \right] \leftrightarrow \left[W, \tilde{k}, \sqrt{E}, \sqrt{H - E} \right]. \quad (\text{A.9})$$

This states that the metamaterial slab can be viewed as an effective rectangular barrier with width L and height $Z_A^2 + \tilde{Z}_B^2$. Different from the quantum case, the barrier height is now strongly dispersive because of the fast variation of the effective mass density of the metamaterial.

References

- [1] J.V. Sanchez-Perez, D. Caballero, R. Martinez-Sala, C. Rubio, J. Sanchez-Dehesa, F. Meseguer, J. Llinares, F. Galvez, Phys. Rev. Lett. 80 (1998) 5325.
- [2] M. Kafesaki, M.M. Sigalas, N. Garcia, Phys. Rev. Lett. 85 (2000) 4044.
- [3] C. Qiu, Z. Liu, J. Mei, J. Shi, Appl. Phys. Lett. 87 (2005) 104101.
- [4] F. Cervera, L. Sanchez, J.V. Sanchez-Perez, R. Martinez-Sala, C. Rubio, F. Meseguer, C. Lopez, D. Caballero, J. Sanchez-Dehesa, Phys. Rev. Lett. 88 (2002) 023902.
- [5] S. Yang, J.H. Page, Z. Liu, M.L. Cowan, C.T. Chan, P. Sheng, Phys. Rev. Lett. 93 (2004) 024301.
- [6] H. Sanchis-Alepuz, Y.A. Kosevich, J. Sanchez-Dehesa, Phys. Rev. Lett. 98 (2007) 134301.
- [7] Z. He, S. Peng, F. Cai, M. Ke, Z. Liu, Phys. Rev. E 76 (2007) 056605.
- [8] X.D. Zhang, Z.Y. Liu, Phys. Rev. Lett. 101 (2008) 264303.
- [9] T.E. Hartman, J. Appl. Phys. 33 (1962) 3427.
- [10] H.G. Winful, Phys. Rev. Lett. 91 (2003) 260401.
- [11] X. Chen, C.-F. Li, Eur. Phys. Lett. 82 (2008) 30009.
- [12] A.M. Steinberg, P.G. Kwiat, R.Y. Chiao, Phys. Rev. Lett. 71 (1993) 708.
- [13] Ch. Spielmann, R. Szepocz, A. Sting, F. Krausz, Phys. Rev. Lett. 73 (1994) 2308.
- [14] M. Mojahedi, E. Schamiloglu, F. Hegeler, K.J. Malloy, Phys. Rev. E 62 (2000) 5758.
- [15] D.L. Solli, J.J. Morehead, C.F. McCormick, J.M. Hickman, J. Opt. A 10 (2008) 075204.
- [16] S.X. Yang, J.H. Page, Z.Y. Liu, M.L. Cowan, C.T. Chan, P. Sheng, Phys. Rev. Lett. 88 (2002) 104301.
- [17] W.M. Robertson, J. Ash, J.M. McCaugh, Amer. J. Phys. 70 (2002) 689.
- [18] Z. Liu, X. Zhang, Y. Mao, Y. Zhu, Z. Yang, C. Chan, P. Sheng, Science 289 (2000) 1734.
- [19] N. Fang, D. Xi, J. Xu, M. Ambati, W. Srituravanich, C. Sun, X. Zhang, Nat. Mater. 5 (2006) 452.
- [20] J. Li, C.T. Chan, Phys. Rev. E 70 (2004) 055602(R).
- [21] Y. Ding, Z. Liu, C. Qiu, J. Shi, Phys. Rev. Lett. 99 (2007) 093904.
- [22] X. Ao, C.T. Chan, Phys. Rev. B 80 (2009) 235118.
- [23] S.H. Lee, C.M. Park, Y.M. Seo, Z.G. Wang, C.K. Kim, Phys. Rev. Lett. 104 (2010) 054301.
- [24] Z. Liu, C.T. Chan, P. Sheng, A.L. Goertzen, J.H. Page, Phys. Rev. B 62 (2000) 278.
- [25] V. Laude, Y. Achaoui, S. Benchabane, A. Khelif, Phys. Rev. B 80 (2009) 092301.